Removal of Cr(vi) and *p*-chlorophenol and generation of electricity using constructed wetland-microbial fuel cells based on *Leersia hexandra* Swartz: *p*-chlorophenol concentration and hydraulic retention time effects†

Yian Wang, [ID] [ab] Xuehong Zhang [ab] and Hua Lin*[ab]

Heavy metals and phenolic compounds existing in polluted wastewater are a threat to the environment and human safety. A downflow *Leersia hexandra* Swartz constructed wetland-microbial fuel cell (DLCW–MFC) was designed to treat polluted wastewater containing Cr(vi) and *p*-chlorophenol (4-CP). To determine the effect of 4-CP concentration and hydraulic retention time (HRT) on the performance of the DLCW–MFC system, the wastewater purification, electricity generation, electrochemical performance, and *L. hexandra* growth status were studied. Addition of 17.9 mg L^{-1} 4-CP improved the power density (72.04 mW m^{-2}) and the charge transfer capacity (exchange current, 4.72×10^{-3} A) of DLCW–MFC. The removal rates of Cr(vi) and 4-CP at a 4-CP concentration of 17.9 mg L^{-1} were 98.8% and 38.1%, respectively. The Cr content in *L. hexandra* was 17.66 mg/10 plants. However, a 4-CP concentration of 35.7 mg L^{-1} inhibited the removal of Cr(vi) and the growth of *L. hexandra*, and decreased the electricity generation (2.5 mW m^{-2}) as well as exchange current (1.21×10^{-3} A) of DLCW–MFC. An increase in power density and removal of Cr(vi) and 4-CP, along with an enhanced transport coefficient of *L. hexandra*, was observed with HRT. At an optimal HRT of 6.5 d, the power density, coulomb efficiency, and exchange current of DLCW–MFC were 72.25 mW m^{-2}, 2.38%, and 4.99×10^{-3} A, respectively. The removal rates of Cr(vi) and 4-CP were 99.0% and 78.6%, respectively. The Cr content and transport coefficient of *L. hexandra* were 4.56 mg/10 plants and 0.451, respectively. Thus, DLCW–MFC is a promising technology that can be used to detoxify polluted wastewater containing composite mixtures and synchronously generate electricity.

1. Introduction

In practice, both Cr(vi) and *p*-chlorophenol (4-CP) are present in industrial wastewater. Chromium in water exists as Cr(iii) and Cr(vi) forms. Cr(vi) is highly soluble and mutagenic compared with Cr(iii), thereby inducing severe toxicity in plants and humans.[1] 4-CP is the typical refractory chlorophenol found in water as a pollutant, which can adversely affect human health. Studies have investigated the toxicity of Cr(vi) and 4-CP. Currently, electrochemical treatment, nanofiltration and advanced oxidation are the methods primarily used to treat Cr(vi) and polluted water containing composite mixtures of

phenolic compounds.[2–4] However, these treatment methods are expensive and complex for large-scale application.

Constructed wetland (CW) is effective in removing phenols or Cr(vi).[5,6] The hyperaccumulator *Leersia hexandra* has been used to remove Cr.[7] Liu *et al.* found that the lack of electrons reduces the efficiency of Cr(vi) reduction to Cr(iii), which decreases the Cr(vi) direct removal rate by *L. hexandra* and thus diminishes the chromium removal efficiency of *L. hexandra* CW.[8] The emergence of microbial fuel cell (MFC) technology is expected to facilitate Cr(vi) reduction. MFC is effective in removing 4-CP, phenol or Cr(vi), and phenol is the main dechlorination product of 4-CP.[9–11] Therefore, the combination of CW and MFC (CW–MFC) has been used to treat single pollutants.[12,13] Fang *et al.* utilized CW–MFC to treat azo dyes at a power density of 11.8 mW m^{-2}, and the azo dye decolorization efficiency was 91.05%.[14] Studies also used other technologies such as biofilm electrode reactor-MFC and photocatalytic-MFC to treat refractory organics and synchronize electricity generation.[15,16] These methods are usually used to treat single refractory organic compounds or heavy metals and are limited in their

a College of Environmental Science and Engineering, Guilin University of Technology, 319 Yanshan Street, Guilin 541000, China. E-mail: linhua5894@163.com

b Guangxi Collaborative Innovation Center for Water Pollution Control and Water Safety in Karst Areas, Guilin University of Technology, 319 Yanshan Street, Guilin 541000, China

† Electronic supplementary information (ESI) available. See https://doi.org/10.1039/d2ra01828d

application for detoxification of aqueous environments containing composite mixtures of heavy metals and phenolic compounds.

Miran *et al.* reported that the 10–100 mg L^{-1} 4-CP removal rate was approximately 40% and yielded electricity under different 4-CP concentrations and lactate as carbon sources in the MFC anode chamber.[17] Phenol can be used as the only fuel for MFC electricity generation; however, the power output was only 6 mW m^{-2}. The co-matrix type including glucose and phenol, azo dye and glucose as carbon sources can be used to improve electricity generation.[15,18] Co-substrates such as glucose and sodium acetate are essential because electricigens cannot directly degrade refractory substances to generate electricity. The presence of a co-substrate facilitates electricity generation and ensures stability of the coupled system.

A high concentration of phenolic pollutants inhibits plant growth *via* endogenous regulation of auxin transport and enzymatic performance. It inhibits microbial activity and survival by denaturing proteins and destroying cell membranes.[19,20] The growth and photosynthetic capacity of plants can affect functions such as release of oxygen, heavy metal enrichment and transfer, which affect the ability of CW–MFC to generate electricity and remove pollutants.[21,22] Experiments were carried out at specific 4-CP concentrations controlling the total COD for effective removal of Cr(VI) and 4-CP and electricity generation. To ensure the stability of the system, it is necessary to reduce the levels of sodium acetate during electricity generation using CW–MFC and prevent the waste of resources when 4-CP is used as a co-substrate. Therefore, the concentration of 4-CP is one of the critical factors determining Cr(VI) and 4-CP treatment. Hydraulic retention time (HRT) affects the performance of CW and MFC. HRT affects the bacterial community at the CW–MFC anode biofilm and the contact time between microorganisms and wastewater.[23] Based on previous studies, it is useful to investigate whether downflow *L. hexandra*-based constructed wetland-microbial fuel cell (DLCW–MFC) can be used to effectively treat polluted water containing Cr(VI) and 4-CP composites.

In present study, simultaneous Cr(VI) and 4-CP removal by DLCW–MFC was proposed using a combination of bio-electrochemical reduction, matrix adsorption, *L. hexandra* enrichment and microbial methods. The effect of each critical parameter including 4-CP concentration and HRT on the treatment of polluted wastewater containing Cr(VI) and 4-CP composites was analyzed to ensure electricity generation. Toward this end, we analyzed the performance of DLCW–MFC in terms of electricity generation, electrochemical changes, water quality, plant physiology and biochemical response, as well as Cr enrichment.

2. Materials and methods

2.1 System setup

The graphite felt (Beijing Jinglongtetan Graphite Factory, Beijing, China) was used to prepare the electrodes including a 2 cm-thick cathode with a 256 cm^2 surface and an anode with a 64 cm^2 surface. They were soaked in 0.1 mol L^{-1} HCl for 24 h to remove oil stains and metal ion pollutants on the surface, and cleaned with distilled water. A cheap stainless steel wire mesh (5 mesh 304 stainless steel wire mesh, 0.6 mm steel wire diameter) was used as a collector soaked in 1 mol L^{-1} H$_2$SO$_4$ solution for 4 h to remove the surface passivation layer.[24] Stainless steel wire mesh was made into a square with sides measuring 8 cm each and buried in the anode. It was also made into a size to wrap the cathode (Fig. 1).

A cylinder measuring 21 cm in diameter and 42 cm in height was used to construct DLCW–MFC (Fig. 1), with an effective height of 28 cm. Gravels measuring 0.3 to 0.6 cm in diameter were used as the support layer weighing 14.15 ± 0.15 kg in total. The packing height was 26 cm, which improved the distribution of wastewater and played a supporting role.[25] The total effective liquid volume of the system was 2.6 ± 0.05 L. As a spacer layer with 10 mm thickness and 21 cm diameter, the glass fiber wool prevents oxygen diffusion from cathode to anode.[26] Cylindrical stainless steel mesh screens (10 mesh, thickness 0.5 mm, no gravel inside the screen) measuring 3 cm in diameter and 8 cm in height were inserted into the cathode area on the left and right sides. Twenty pre-cultured *L. hexandra* plants were planted into the cylindrical stainless steel mesh screens.[27] A closed circuit was formed by a copper wire (1 mm diameter) connected to an anode and a cathode, with a resistance of 2000 Ω.[28] The liquid level was maintained at the lower surface of the cathode to form an air cathode.

2.2 Inoculation and initiation of CW–MFC

Sludge was obtained from the Qilidian sewage treatment plant (Guilin, China). It was used as the original inoculum in the DLCW–MFC system. The sludge (7 g L^{-1}) was inoculated from the bottom of the system and filled to the lower surface of the cathode. The system was operated stably for more than three months before commencing the experiment. After inoculation, the synthetic solution was continuously pumped through the peristaltic pump (Leifu BT101L DG10-2, Baoding, China) at 25 ± 2 °C. The basic ingredients of the 1 L synthetic solution included 5 mM phosphate buffer solution, 0.1132 g K$_2$Cr$_2$O$_7$, 0.15 g NH$_4$Cl, 0.13 g KCl and 1 mL micronutrient solution. The preparation of micronutrient solution was reported previously.[29] Different 4-CP concentrations of wastewater were obtained using 4-CP and sodium acetate under a total COD of 300 mg L^{-1}. The pH of the influent synthetic solution was adjusted to 6.5 ± 0.1. The different operational conditions of DLCW–MFC are shown in Table 1.

2.3 Electrochemical performance

The output voltage was determined every 30 min using Lab-Quest mini host and voltage sensor DVP-BTA (Vernier Software & Technology, USA). The anode and cathode potentials were measured using a multimeter (Fluke F18B, Fluke Corporation, USA). The power density curve was measured based on the voltage after 30 min by adjusting the different resistance values. The coulomb efficiency (CE), defined as the fraction of electrons used for electricity generation *versus* the electrons in the starting organic matter, was calculated as described in a previous
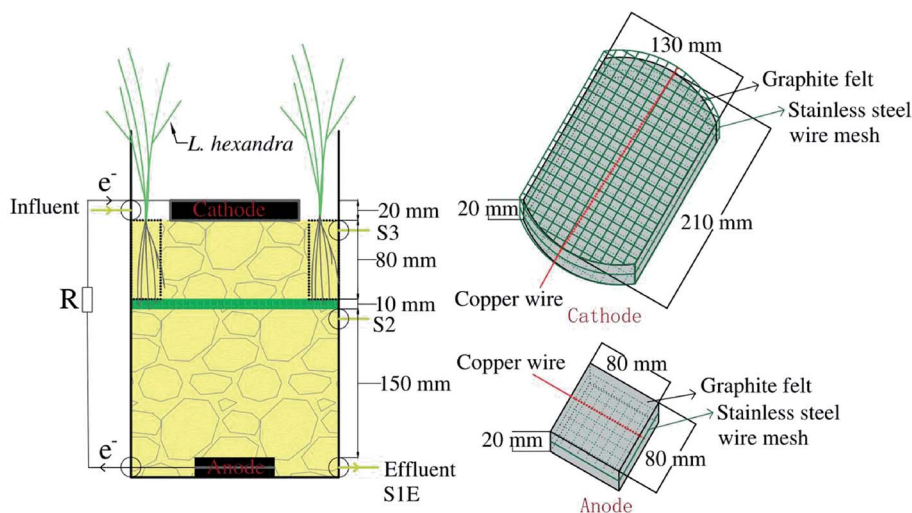
Fig. 1 DLCW−MFC structure diagram (S1, S2 and S3 were sample taps, and the suffix E represents effluent tap).

Table 1 The different operational conditions of DLCW−MFC

	Stage 1	Stage 2	Stage 3	Stage 4	Stage 5	Stage 6
4-CP concentration (mg L^{-1})	0	17.9	35.7	35.7	35.7	35.7
Sodium acetate concentration (mg L^{-1})	384.5	346.1	307.6	307.6	307.6	307.6
HRT (d)	1.5	1.5	1.5	2.5	4.5	6.5

study.[30] A three-electrode system of CHI604E electrochemical workstation (Shanghai Chenhua Instrument Co., Ltd., Shanghai, China) was used to perform electrochemical impedance spectroscopy (EIS) as well as construct the cyclic voltammetry (CV), linear sweep voltammetry (LSV), and Tafel (TAF) curves. The CV potential scan speed was 30 mV s^{-1}. The LSV potential scan range was 0–1.0 V, and the scan speed was 30 mV s^{-1}. The scanning voltage of TAF was −2.0 to 1.0 V and the scan speed was 10 mV s^{-1}. The linear fitting was performed in the over-potential range of 0.3–0.5 V,[31] and the calculated exchange current (i_0) was calculated by extrapolating the TAF curve to 0 V overpotential. EIS was performed at 10 kHz to 1 mHz and 5 mV alternating current signal. The equivalent circuit $R(Q(RW))$ was fitted with the EIS results. The Nyquist plot was analyzed using the Nova 2.1.4 software.

2.4 Water quality analysis

The COD, Cr(VI), total Cr (TCr) and 4-CP levels in the water samples were determined from the S1E sample tap. The COD (without filtration) was measured using the Hach's COD digestion instrument (DRB200, HACH, USA) and COD instrument (DR1010, HACH, USA). The Cr(VI) content in the water was determined via diphenylcarbonyl hydrazine spectrophotometry with a maximum absorbance at 540 nm. The TCr in the water was digested with a 10 mL mixture of H_2SO_4 and HNO_3 (1 : 1, v/v) at 120 °C and analyzed with an atomic absorption spectrophotometer (TAS-990F, PERSEE, Beijing, China).[8] The water samples obtained from S1E, S2 and S3 sample taps were used to measure the oxidation–reduction potential (ORP) using the

S210-S benchtop pH meter (Mettler Toledo, Switzerland). The water samples from the S3 sample tap were used to determine the hydrogen peroxide (H_2O_2) content using the H_2O_2 content detection kit (Solarbio Life Sciences, Beijing, China). These water sample measurements were performed in triplicate after determining the electrochemical performance indices.

The 4-CP content was determined via high performance liquid chromatography (HPLC) (LC-2030C-3DPLUS, SHIMADZU, Japan). A symmetric C-18 column (5 μm, 4.6 × 250 mm column) was used at a temperature of 30 °C. A methanol/water mixture (70 : 30, v/v) was used as the mobile phase. The mobile phase flow rate was 1 mL min^{-1} during the analysis, and the sample injection volume was 20 μL. The detection was performed at 280 nm.[17] The standard sample of 2 g L^{-1} 4-CP was filtered with 0.45 μm PVDF and PTFE filtration membranes (Tianjin Jinteng Experimental Equipment Co., LTD., China) to analyze the role of filter membrane. An appropriate filter membrane was selected to determine the 4-CP content in the effluent (S1E sample tap) of DLCW−MFC.

2.5 Physiological and biochemical response and Cr enrichment of *L. hexandra*

The planting cycle of *L. hexandra* was 15 d. The plants were divided into roots, stems and leaves after cleaning. The root was cleaned with 10 mmol L^{-1} EDTA–Na$_2$ using an ultrasonic cleaner to desorb the heavy metals on the root surface. Each tissue was dried at 105 °C for 30 min and then at 70 °C to constant weight to measure the plant height, root length and biomass (dry weight).[32] A 0.5 g tissue sample was heated and
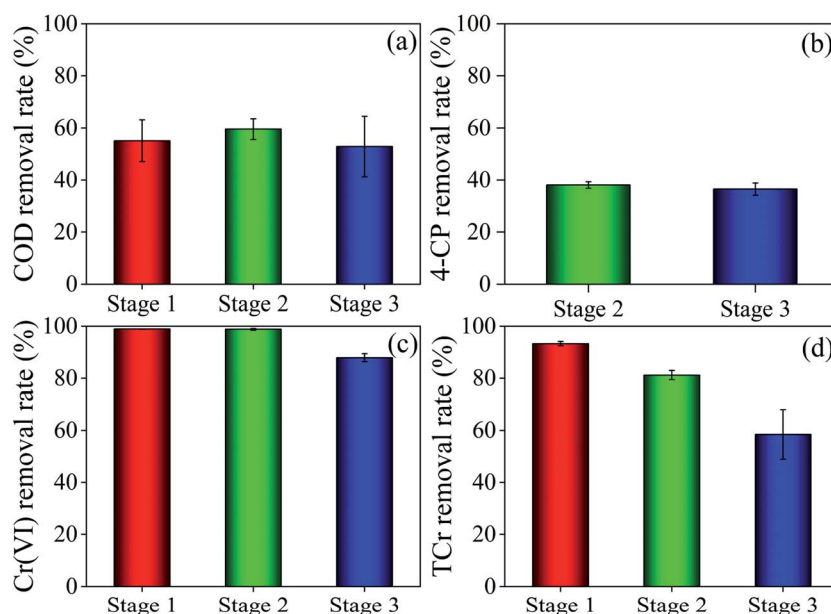
Fig. 2   (a) COD, (b) 4-CP, (c) Cr(VI) and (d) TCr removal rates at different concentrations of 4-CP.
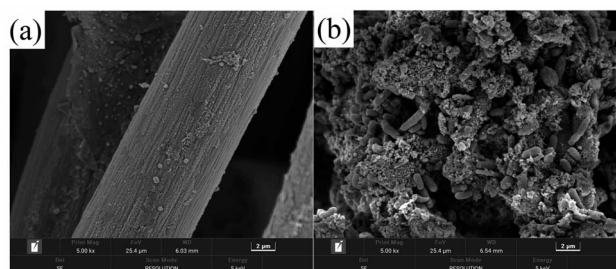

Fig. 3   SEM image of (a) raw graphite felt and (b) anode biofilm of the DLCW–MFC.

digested with 15 mL aqua regia to determine Cr content using TAS-990F, and the transport coefficient (TF) was calculated as described in a previous study.[33] The Cr enrichment in above-ground and underground parts was calculated based on the tissue biomass. 0.1 g of fresh leaves were used to measure the chlorophyll a, chlorophyll b and carotenoid levels of *L. hexandra* using the acetone method.[34] The total phenolic content of the plant leaves was determined using the Folin–Ciocalteu method.[35]

3.   Results and discussion

3.1   Effects of 4-CP concentrations on wastewater treatment, electricity generation and *L. hexandra* growth

The effects of 4-CP concentration on the COD, 4-CP, Cr(VI) and TCr removal rates were investigated (Fig. 2). The Cr(VI) removal rates at stages 1, 2 and 3 were 98.9%, 98.8% and 87.9%, respectively, while the TCr removal rates were 93.3%, 81.2% and 58.5%, respectively, indicating that high concentrations of 4-CP inhibited the removal of Cr(VI) and TCr. The high concentration

of phenolic compounds inhibits the growth and activity of plants and microorganisms.[36,37] The 4-CP removal rate was 36.5% at stage 3, which was lower than in stage 2, due to the decreased removal efficiency of Cr(VI) and TCr, and the negative effects caused by the high concentration of 4-CP. The COD removal rate at stage 2 (59.6%) was slightly higher than at stage 1 (55.1%) and stage 3 (52.9%), which may be attributed to the low concentration of phenolic compound stimulating the growth of plants and microorganisms to promote electricity generation and the degradation of organic matter.[38–40] The 4-CP acts as an oxidant and therefore the ORP of each sample tap at stage 3 was higher than at stages 1 and 2. Removal of Cr(VI) and 4-CP led to a decline in ORP along the route (Fig. S2†). The ORP of S1E sample tap at stages 1, 2 and 3 was −83.4 mV, −97.6 mV and 100.5 mV, respectively, indicating stronger detoxification of Cr(VI) and 4-CP composites in the polluted water at stage 2 than at stage 3.

Electricigens can be used as biocatalysts to oxidize carbon sources and promote electricity generation. The presence of multiple grooves on the raw graphite felt surface facilitates bacterial growth and the formation of an effective electrical biofilm on the electrode surface (Fig. 3). Electrochemical performance and electricity generation were analyzed to explore the effect of different 4-CP concentrations on the bioelectric output of DLCW–MFC. CV and LSV curves (Fig. S3a and b†) indicate that low concentrations of 4-CP enhanced the current response and charge transfer capacity of the system anode, because 4-CP is an electron receptor.[9] Influx of water at the cathode reduced the effect of cathode polarization. However, a high concentration of 4-CP inhibited the electron transfer capacity and current response, because the water pollutants cannot be effectively removed within the short HRT, resulting in serious toxicity. TAF curves (Fig. S3c†) show that the exchange
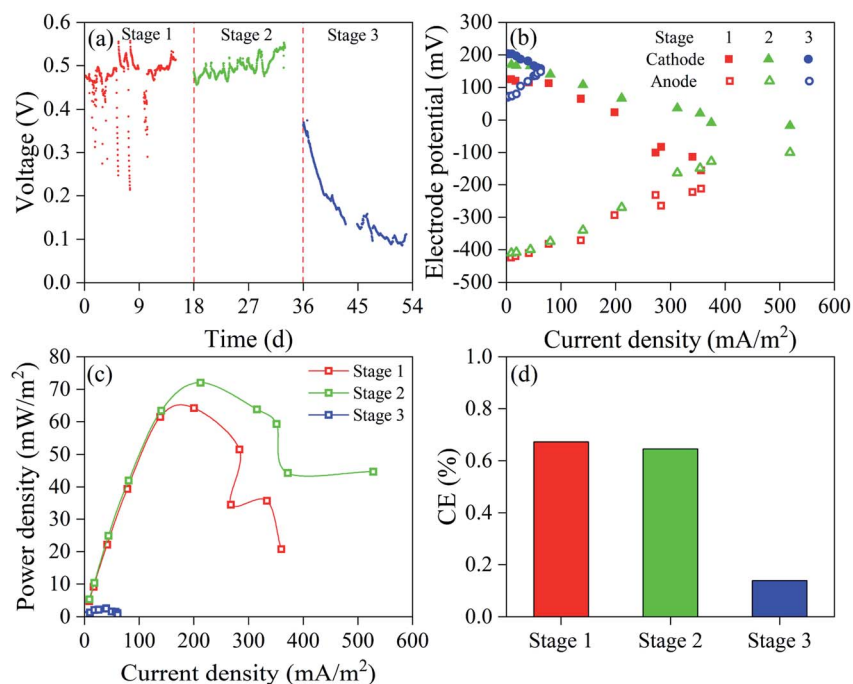
Fig. 4 (a) Output voltage, (b) cathode and anode potential, (c) power density curves and (d) CE at different concentrations of 4-CP.

current (i_0) at stage 2 was 4.72×10^{-3} A, which was higher than at stage 1 (4.63×10^{-3} A) and stage 3 (1.21×10^{-3} A), indicating higher kinetic activity of the anode at low concentrations of 4-CP. The results of EIS (Fig. S3d†) show that the solution resistance (R_s) plus charge transfer resistance (R_p) at stage 2 was 71.3 Ω, which was lower than at stage 1 (77.8 Ω) and stage 3 (75.1 Ω). The Warburg impedance diffusion resistance (W) at stages 1, 2 and 3 was 0.48×10^{-3} Ω, 0.55×10^{-3} Ω and 0.58×10^{-3} Ω, respectively. The 4-CP may form larger ionic radii and greater steric hindrance during movement, compared with sodium acetate.[41,42] The viscosity of 4-CP is higher than that of sodium acetate, which decreases the local motion and hinders ion diffusion.[43] These results show that the diffusion of ions generated in the system at the electrode interface is attenuated and the charge transfer was inhibited by the increased 4-CP concentration.

As shown in Fig. 4a, the electricity generation by DLCW–MFC at stages 1 and 2 (>500 mV) was better than at stage 3. Anode electricigens can degrade organic compounds such as phenol and sodium acetate to obtain electrons,[18] reaching the cathode *via* an external circuit to generate voltage. Under similar high current density, the anode potential at stage 2 was lower, while the cathode potential was higher (Fig. 4b), which is attributed to the oxidizing effects of Cr(VI) and 4-CP and effective utilization of electrons at the cathode, thus slowing down the cathode polarization effect. The decrease in cathode polarization improves the output power density, and the maximum output power density at stage 2 was 72.0 mW m^{-2} (Fig. 4c), higher than at stage 1 (64.2 mW m^{-2}) and stage 3 (2.5 mW m^{-2}). Miran *et al.* reported that an excessively high concentration of 4-CP inhibits the electricity generation of MFC.[17] The system anode had a higher potential at stage 3, indicating accumulation of
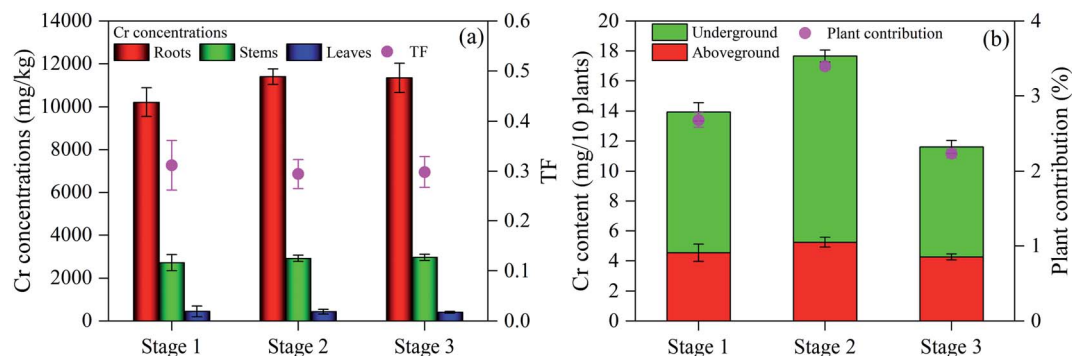

Fig. 5 (a) Cr concentrations in roots, stems and leaves and TF and (b) Cr content in aboveground and underground parts of *L. hexandra* at different concentrations of 4-CP.
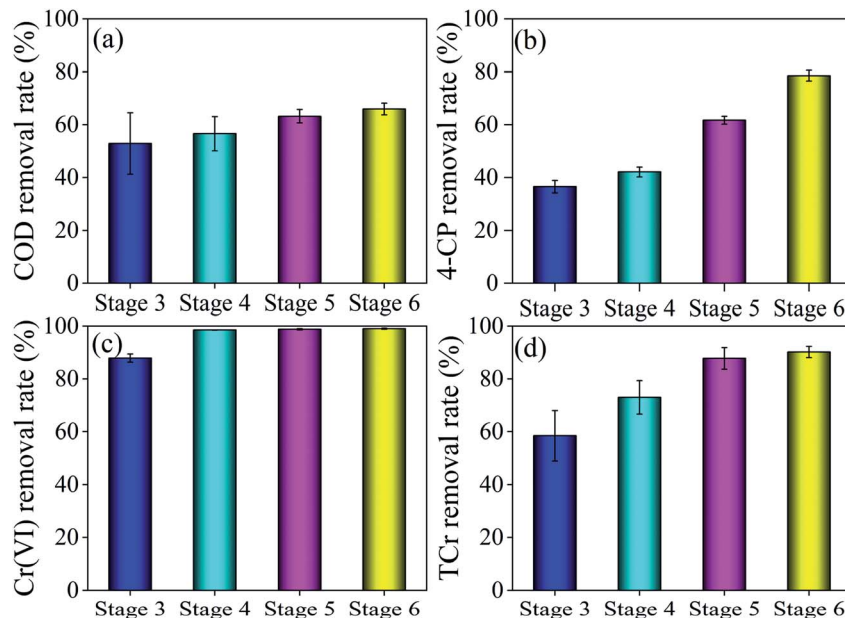
Fig. 6 (a) COD, (b) 4-CP, (c) Cr(VI) and (d) TCr removal rates at different HRT.

excessive positive charge in the anode, and the electricigens were exposed to specific toxic effects. Therefore, the difference in power density between stages 1 and 2 was mainly induced by the cathode performance, and the anode potential played a major role in power output at stage 3. At stage 3, the H_2O_2 content at the cathode (Fig. S4†) decreased to 4.59 mg L^{-1}, mainly due to declining power generation capacity.[44] 4-CP is oxidized and degraded by H_2O_2 and undergoes dechlorination

by accepting electrons,[17,45] while Cr(VI) can be reduced by the electrons and H_2O_2,[1,46] further indicating that the inhibition of electricity generation reduced the detoxification efficiency of the polluted water. The CE at stage 3 (Fig. 4d) was 0.14%, which was lower than at stage 1 (0.67%) and stage 2 (0.65%), indicating that the rate of utilization of organic matter by electricigens at stage 3 was low. By contrast, CE was only 0.1–0.3% in previous CW–MFC studies.[30] Khan *et al.* reported that the
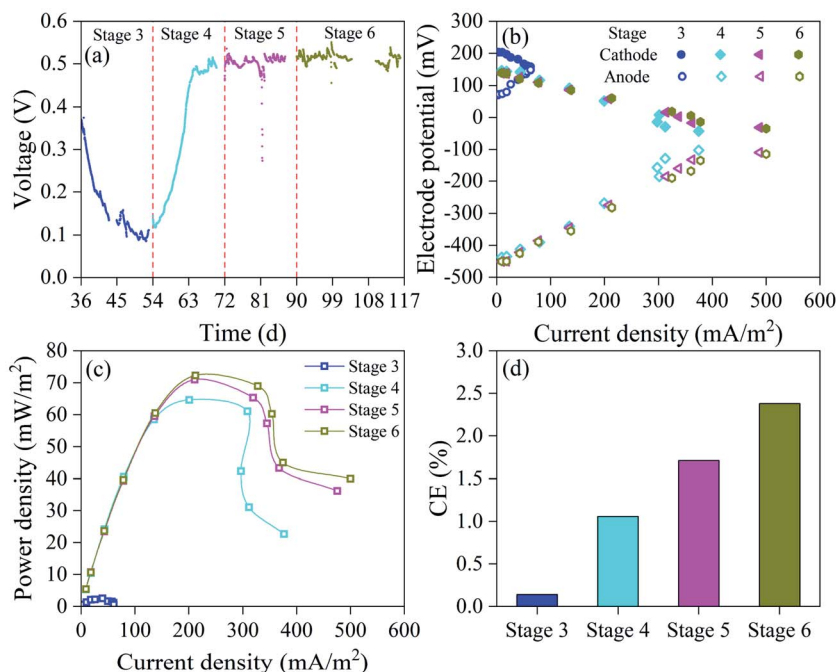

Fig. 7 (a) Output voltage, (b) cathode and anode potential, (c) power density curves and (d) CE at different HRT.
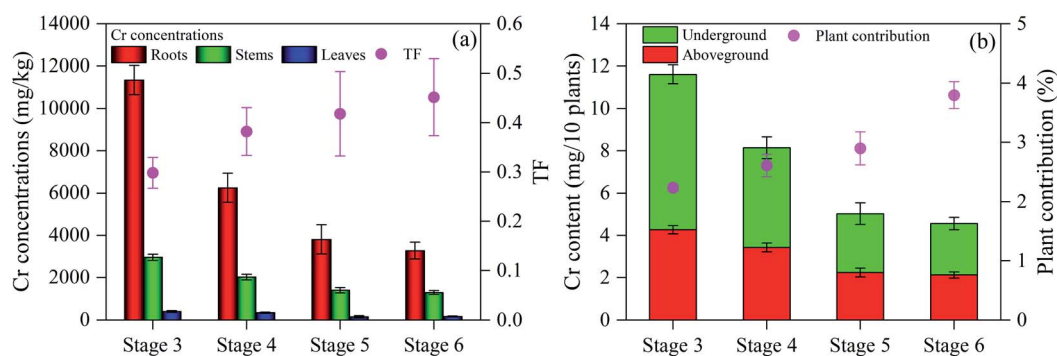
Fig. 8 (a) Cr concentrations in roots, stems and leaves and TF and (b) Cr content in aboveground and underground parts of *L. hexandra* at different HRT.

presence of phenol at the cathode of double-chamber MFC enhanced electron flux and enhanced the power output; however, the output power density decreased with the increased phenol levels, thereby slowing down the overall system performance.[10] This phenomenon was similar to stages 2 and 3 in this study.

To effectively recover the heavy metals from the polluted water, the *L. hexandra* plants were included in the cathode area of DLCW–MFC to enrich Cr.[32] As shown in Fig. S5,† the total phenol content of *L. hexandra* leaves at stages 1, 2 and 3 was 2.77, 3.20 and 2.22 mg g^{-1}, respectively. Generally, the antioxidant activity of plants is positively correlated with the total phenol content *in vivo*.[47] Total phenols can inhibit the conversion of hydrogen peroxide to reactive oxygen species and promote defense mechanisms to resist toxicity.[48] Compared with stages 1 and 3 (Fig. S6†), stage 2 showed improvement in plant height, root length, and dry weight of each tissue of *L. hexandra*, indicating that low phenolic concentrations promoted plant growth. This result was similar to the growth reported by Ibáñez *et al.*[39] With the increase of 4-CP concentration, the toxic effect generated a large number of reactive oxygen species (ROS), which triggered oxidative damage of plants and damaged protein and chlorophyll structure and function.[49] The levels of chlorophyll a, chlorophyll b and

carotenoids at stage 3 decreased by 39.8%, 57.4% and 14.3%, respectively, compared with those at stage 2. Toxic effects reduce the levels of chlorophyll a, chlorophyll b and carotenoids,[50] thereby inhibiting plant photosynthesis and growth.

The Cr concentrations in roots, stems and leaves of *L. hexandra* at stage 2 were 11 401, 2915 and 434 mg kg^{-1}, respectively (Fig. 5a), higher than at stage 1 at 10 214, 2717 and 454 mg kg^{-1}, respectively and at stage 3 at 11 343, 2960 and 408 mg kg^{-1}, respectively. These results were higher than those reported previously including an underground Cr concentration of 785 mg kg^{-1} and an aboveground level of 297 mg kg^{-1}.[7] This result was mainly attributed to the positive Cr(III) absorption of *L. hexandra*.[32] Cr(VI) can be converted to Cr(III) *via* H$_2$O$_2$, electron capture and microbial mechanisms, which accumulate large amounts of Cr in *L. hexandra*. The Cr content of *L. hexandra* at stages 1, 2 and 3 was 13.95, 17.66 and 11.61 mg/10 plants, respectively (Fig. 5b). Accordingly, the contribution to Cr(VI) removal of *L. hexandra* decreased in the following order: stage 2 (3.40%) > stage 1 (2.68%) > stage 3 (2.23%). This is attributed to variation in plant growth status, which resulted in different detoxification outcomes and varying levels of electricity generation.[22] This study further contributes to the practical applications of CW–MFC to treat different types of polluted industrial wastewater. Considering the decline in output voltage to 90–

Table 2 The electricity generation and pollutants removal performance of recent CW–MFC studies

HRT (d)	Substrate	Influent COD (mg L^{-1})	Refractory organics or heavy metals	Voltage (mV)	Power density (mW m^{-2})	Removal rate	Ref.
2.5	Sodium acetate	300	35.7 mg L^{-1} 4-CP and 40 mg L^{-1} Cr(VI)	516	64.6	4-CP: 42.1% Cr(VI): 98.5%	Present study
6.5				543	72.25	4-CP: 78.6% Cr(VI): 99.0%	
4	Glucose	500	60 mg L^{-1} Cr(VI)	545.6	29.8	Cr(VI): 89.6%	52
0.625	Sodium acetate	880	—	27–42	2.016	—	58
3	—	—	10 mg L^{-1} Zn(II)	257	3.87	Zn(II): 98.56%	59
3	Glucose	60	5 mg L^{-1} Pb(II)	343	7.432	Pb(II): 84.86%	57
7.6	Glucose	262	—	—	2–3	—	60
3	Glucose	—	300 mg L^{-1} azo dye ABRX3	342	11.8	ABRX3: 91.05%	14
3	Glucose	426.8	4 mg L^{-1} sulfadiazine	472	15.41	Sulfadiazine: 99.9%	61
0.67	Glucose	426.8	10 mg L^{-1} bisphenol A	420	18.43	Bisphenol A: 91.3%	62

110 mV at stage 3 and the stability, the rate of 4-CP removal at stage 3 was comparable to that at stage 2, which indicates that the presence of electricigens in the system and their tolerance to the influx of synthetic solution containing 35.7 mg L^{-1} 4-CP. Therefore, 35.7 mg L^{-1} 4-CP was selected for subsequent experiments.

3.2 Effects of HRT on wastewater treatment, electricity generation and *L. hexandra* growth

To effectively remove high concentrations of 4-CP and generate electricity synchronously, we prolonged HRT to determine its effect on system performance. The COD, 4-CP, Cr(VI) and TCr removal rates were improved with increased HRT (Fig. 6). The COD, 4-CP, Cr(VI) and TCr removal rates at stage 6 were 66.0%, 78.6%, 99.0% and 90.2%, respectively. Wagner *et al.* reported that a relatively long HRT (5–7 d) contributed to synergistic microbial removal of refractory organic matter.[51] The effective removal of materials oxidized with 4-CP and Cr(VI) decreased the ORP of water (Fig. S7†). The ORP of the S3 sample tap at stage 6 was 28.4 mV, which was lower than at stage 5 (77 mV), indicating that 4-CP and Cr(VI) were removed in large quantities at the cathode at stage 6. The ORP of S1E sample tap at stages 4, 5 and 6 was −106.5 mV, −130.5 mV and −137.5 mV, respectively, which were lower than at stage 3 (100.5 mV). This result indicates significant improvement in the decontamination of wastewater at stage 4, thereby preventing toxic effects on electricigens and improving the electricity generation.

The effect of different HRT levels on biological electricity generation of DLCW–MFC was explored by analyzing the electrochemical performance and electricity generation. Based on CV and LSV curves (Fig. S8a and b†), the current response and charge transfer capability of the anode increased with the increase in HRT, mainly due to the prevention of excessive influx of toxic substances into the anode. TAF curves (Fig. S8c†) show that i_0 at stages 4, 5 and 6 was 4.34×10^{-3} A, 4.99×10^{-3} A and 4.99×10^{-3} A, respectively, indicating that prolonged HRT improved the anode kinetic activity. Studies have shown that the increased HRT can reduce the toxic effects on microorganisms and improve electricity generation by the system.[52] EIS (Fig. S8d†) results indicate that the R_s plus R_p at stage 6 was 71.3 Ω, which was lower than at stages 3–5. The value of W at stages 4, 5 and 6 was 0.39×10^{-3} Ω, 0.39×10^{-3} Ω and 0.41×10^{-3} Ω, respectively, which were lower than at stage 3 (0.58×10^{-3} Ω), mainly due to the effective removal of 4-CP. These results indicate that prolonged HRT increases the diffusion of ions generated in the system to the electrode interface and improve the charge transferability.

Fig. 7a shows that the output voltage was recovered and exceeded 500 mV at stage 4. Under the same high current density, prolonged HRT can reduce the anode potential (Fig. 7b) to increase the potential difference between anode and cathode, and improve the output power density. When the HRT was increased from 2.5 to 4.5 d, the maximum power density increased to 10.0% (Fig. 7c). However, when the HRT increased from 4.5 to 6.5 days, the maximum power density only increased by 1.8% to 72.25 mW m^{-2}. Studies have shown that increased

HRT can increase the utilization of the available organic matter by microbes,[23] thus promoting their growth and reproduction and improving the abundance of electricigens. The increased activity of electricigens generates electrons and improves electron transport capacity, thereby reducing internal resistance and enhancing power density.[53] At stage 4, the H$_2$O$_2$ content at the cathode (Fig. S9†) increased to 5.54 mg L^{-1}, mainly due to improved electricity generation. Yong *et al.* reported that only 4.6 mg L^{-1} of H$_2$O$_2$ was released at the cathode of MFC.[54] The H$_2$O$_2$ content at cathode at stages 5 and 6 was 3.00 mg L^{-1} and 2.71 mg L^{-1}, respectively, mainly due to the increased HRT, which was conducive to the removal of 4-CP and Cr(VI) by H$_2$O$_2$. Thus, a large amount of H$_2$O$_2$ is consumed under conditions of limited dissolved oxygen. The CE (Fig. 7d) at stages 4, 5 and 6 was 1.06%, 1.71% and 2.38%, respectively, further indicating that increased HRT can promote effective utilization of organic matter by electricigens. The CE of this study was substantially larger than in previous studies (0.1–0.3%).[30] Excessive increase in HRT affects plant growth and electron donor supply due to the consumption of available carbon sources. Therefore, an HRT of 6.5 d was expected to improve the treatment performance and electricity generation by DLCW–MFC exposed to Cr(VI) and 4-CP composite polluted wastewater.

The total phenol content at stages 4, 5 and 6 was 8.04, 8.59 and 8.87 mg g^{-1}, respectively (Fig. S10†), indicating that increased HRT improved the total phenol content alleviate stress. Plant height, root length, tissue dry weight and chlorophyll and carotenoid contents were increased at stages 4, 5 and 6, compared with stage 3 (Fig. S11†). Thus, prolonged HRT facilitated the removal of Cr(VI) and 4-CP to alleviate the toxic effects on plants. Studies reported that increased HRT contributes to plant growth and improves their ability to eliminate pollutants, due to slow biodegradation.[55,56] With the increase of HRT, the Cr concentrations in the roots, stems and leaves were decreased (Fig. 8a). When HRT increased to 6.5 d, the Cr concentrations in the roots, stems and leaves were 3279, 1290 and 171 mg kg^{-1}, respectively. The TF of *L. hexandra* at stages 4, 5 and 6 was 0.382, 0.418 and 0.451, respectively, higher than at stage 3 (0.298), and higher than those reported previously (0.1–0.3).[7] The results show a decrease in Cr concentration of each tissue of *L. hexandra*, while the transport capacity improved with increased HRT. The accumulated Cr content of *L. hexandra* at stages 4, 5 and 6 was 8.14, 5.02 and 4.56 mg/10 plant, respectively (Fig. 8b). The contribution to Cr(VI) removal of *L. hexandra* was in the following order: stage 4 (2.61%) < stage 5 (2.90%) < stage 6 (3.80%). This is because different HRTs under the limited experimental period led to variation in the total volume of influent synthetic solution. This study further enhances the role of plants in the recovery of heavy metals, wastewater treatment and available carbon source utilization in DLCW–MFC. Considering that the system had the highest output power density and exhibited excellent treatment performance in eliminating Cr(VI) and 4-CP at stage 6, the growth state of *L. hexandra* at stage 6 decreased slightly compared with stage 5. Therefore, an HRT of 6.5 d was considered as the most appropriate for optimal performance.

3.3 Strengths and limitations

This study is the first of its kind demonstrating the superior performance of downflow *L. hexandra* CW–MFC for the decontamination of polluted wastewater containing Cr(VI) and 4-CP composites and generation of electricity. Compared with other studies (Table 2), our study demonstrates stronger electricity generation and higher detoxification of polluted water containing phenolic compounds and heavy metals. This downflow CW–MFC technology is also superior to other flow patterns of CW–MFC (power density usually less than 30 mW m^{-2}).[30,57]

However, there are two noteworthy limitations: (1) This study did not explore other important factors such as pH or electrode spacing; (2) the role of root exudate of *L. hexandra* in DLCW–MFC remains to be clarified due to secretions that help bacterial growth.

4. Conclusions

Factors such as 4-CP concentration and HRT affect wastewater treatment, electricity generation, plant growth and Cr enrichment. When Cr(VI) concentration was 40 mg L^{-1} and 4-CP concentration was 17.9 mg L^{-1}, the Cr(VI) and 4-CP removal rates were 98.8% and 38.1%, respectively, DLCW–MFC had stronger charge transferability, higher output power density (72.04 mW m^{-2}), acceptable plant growth state and Cr enrichment ability (17.66 mg/10 plants). A high 4-CP concentration (35.7 mg L^{-1}) reduced the electrochemical performance, electricity generation and wastewater treatment capacity of DLCW–MFC, and inhibited the growth and Cr enrichment capacity of *L. hexandra*. A prolonged HRT improved the Cr(VI) and 4-CP removal rates, charge transfer capability and electricity generation by DLCW–MFC. An HRT of 6.5 d resulted in Cr(VI) and 4-CP removal rates of 99.0% and 78.6%, respectively, and the maximum output power density was 72.25 mW m^{-2}. The increased HRT alleviated the stress on *L. hexandra*, and improved its growth, TF (0.451), and the contribution to Cr(VI) removal (3.80%). Therefore, the findings of high output power density, increased rates of Cr(VI) and 4-CP removal, and the physiological and biochemical responses as well as Cr enrichment effects of *L. hexandra* demonstrate the effectiveness of DLCW–MFC technology for successful treatment of polluted wastewaters containing Cr(VI) and 4-CP composites and generate electricity at the same time.

Ethical approval

No applicable.

Consent to participate

No applicable.

Consent to publish

All authors agree to publication.

Data availability

All data and materials generated or analysed during this study are included in this published article (and its ESI†).

Author contributions

Yian Wang: data curation, methodology, software, investigation, writing – original draft. Xuehong Zhang: validation, resources, funding acquisition. Hua Lin: methodology, validation, conceptualization, supervision, funding acquisition. All authors read and approved the final manuscript.

Conflicts of interest

The authors declared that they have no conflicts of interest to this work. We declare that we do not have any commercial or associative interest that represents a conflict of interest in connection with the work submitted.

References

1 S. Zhao, P. Liu, Y. Y. Niu, Z. J. Chen, A. Khan, P. Y. Zhang and X. K. Li, *Sensors*, 2018, **18**, 642.
2 C. L. P. S. Zanta, P. A. Michaud, C. Comninellis, A. R. D. Andrade and J. F. C. Boodts, *J. Appl. Electrochem.*, 2003, **33**, 1211–1215.
3 A. M. Hidalgo, G. León, M. Gómez, M. D. Murcia, E. Gómez and J. L. Gómez, *Desalination*, 2013, **315**, 70–75.
4 A. Yazdanbakhsh, A. Aliyari, A. Sheikhmohammadi and E. Aghayani, *J. Water Proc. Eng.*, 2020, **34**, 101080.
5 A. Mojiri, Z. Ahmad, R. M. Tajuddin, M. F. Arshad and A. Gholami, *Environ. Monit. Assess.*, 2017, **189**, 337.
6 G. Dotro, D. Larsen and P. Palazolo, *Water Environ. J.*, 2011, **25**, 241–249.
7 C. Wang, H. Tan, H. Li, Y. L. Xie, H. K. Liu, F. Xu and H. Xu, *Environ. Pollut.*, 2020, **257**, 113558.
8 J. Liu, X. H. Zhang, S. H. You, Q. X. Wua and K. N. Zhou, *Ecol. Eng.*, 2015, **81**, 70–75.
9 H. Y. Gu, X. W. Zhang, Z. J. Li and L. C. Lei, *Chin. Sci. Bull.*, 2007, **52**, 3448–3451.
10 N. Khan, A. H. Anwer, A. Ahmad, S. Sabir, S. Sevda and M. Z. Khan, *ACS Omega*, 2020, **5**, 471–480.
11 M. Sindhuja, S. Harinipriya, A. C. Bala and A. K. Ray, *J. Hazard. Mater.*, 2018, **355**, 197–205.

12 L. Wang, D. Xu, Q. Zhang, T. Liu and Z. Tao, *Environ. Sci. Pollut. Res.*, 2022, **29**, 768–778.

13 H. Li, H. L. Song, X. L. Yang, S. Zhang, Y. L. Yang, L. M. Zhang, H. Xu and Y. W. Wang, *Sci. Total Environ.*, 2018, **637–638**, 295–305.

14 Z. Fang, S. Cheng, X. Cao, H. Wang and X. Li, *Environ. Technol.*, 2017, **38**, 1051–1060.

15 X. Cao, S. Zhang, H. Wang and X. N. Li, *Chemosphere*, 2019, **216**, 742–748.

16 C. Z. Wang, G. L. Wu, X. L. Zhu, Y. Xing, X. Yuan and J. Qu, *Chemosphere*, 2022, **293**, 133517.

17 W. Miran, M. Nawaz, J. Jang and D. S. Lee, *Water Res.*, 2017, **117**, 198–206.

18 H. P. Luo, G. L. Liu, R. D. Zhang and S. Jin, *Chem. Eng. J.*, 2009, **147**, 259–264.

19 H. Rasouli, M. H. Farzaei, K. Mansouri, S. Mohammadzadeh and R. Khodarahmi, *Mol*, 2016, **21**, 1104.

20 S. E. Agarry, A. O. Durojaiye and B. O. Solomon, *Int. J. Environ. Pollut.*, 2008, **32**, 12–28.

21 A. Dziwulska-Hunek, M. Ćwintal, A. Niemczynowicz, B. Boroń and A. Matwijczuk, *Pol. J. Environ. Stud.*, 2019, **28**, 3133–3143.

22 Y. Yang, Y. Q. Zhao, C. Tang, R. B. Liu and T. H. Chen, *Chemosphere*, 2021, **263**, 128354.

23 G. Z. Wang, Y. T. Guo, J. Y. Cai, H. Y. Wen, Z. Mao, H. Zhang, X. Wang, L. Ma and M. Q. Zhu, *RSC Adv.*, 2019, **9**, 21460–21472.

24 X. W. Peng, S. L. Chen, L. Liu, S. Q. Zheng and M. Li, *Electrochim. Acta*, 2016, **194**, 246–252.

25 L. Xu, Y. Q. Zhao, L. Doherty, Y. S. Hu and X. D. Hao, *Sci. Rep.*, 2016, **6**, 26514.

26 L. Xu, Y. Q. Zhao, C. Tang and L. Doherty, *J. Environ. Manage.*, 2018, **207**, 116–123.

27 X. H. Zhang, J. Liu, D. Q. Wang, Y. N. Zhu, C. Hu and J. J. Sun, *Bull. Environ. Contam. Toxicol.*, 2009, **82**, 358–362.

28 Y. T. Guo, G. Z. Wang, H. Zhang, H. Y. Wen and W. Li, *Biotechnol. Biofuels*, 2020, **13**, 162.

29 S. T. Liu, H. L. Song, S. Z. Wei, F. Yang and X. N. Li, *Bioresour. Technol.*, 2014, **166**, 575–583.

30 L. Doherty, X. H. Zhao, Y. Q. Zhao and W. K. Wang, *Ecol. Eng.*, 2015, **79**, 8–14.

31 N. M. Noor, R. Othman, M. A. M. Hatta and M. H. Ani, *Int. J. Electroactive Mater.*, 2014, **2**, 22–27.

32 X. H. Zhang, J. Liu, H. T. Huang, J. Chen, Y. N. Zhu and D. Q. Wang, *Chemosphere*, 2007, **67**, 1138–1143.

33 E. D. Udosen, N. U. Benson, J. P. Essien and G. A. Ebong, *Int. J. Soil Sci.*, 2006, **1**, 27–32.

34 U. A. Seyrek, M. Luo, M. Zhong, C. H. Huang, J. J. Tao, X. Y. Qu and X. B. Xu, *Agric. Sci.*, 2017, **8**, 465–478.

35 Z. Zargoosh, M. Ghavam, G. Bacchetta and A. Tavili, *Sci. Rep.*, 2019, **9**, 16021.

36 R. Chen, L. F. Ren, J. H. Shao, Y. L. He and X. F. Zhang, *RSC Adv.*, 2017, **7**, 52841–52851.

37 K. Wang, J. Cai, J. Feng and S. L. Xie, *Environ. Monit. Assess.*, 2014, **186**, 8667–8681.

38 S. Pontigo, M. Ulloa, K. Godoy, N. Nikolic, M. Nikolic, M. d. l. L. Mora and P. Cartes, *J. Soil Sci. Plant Nutr.*, 2018, **18**, 904–920.

39 S. G. Ibáñez, L. G. S. Alderete, M. I. Medina and E. Agostini, *Environ. Sci. Pollut. Res.*, 2012, **19**, 1555–1562.

40 L. Doherty, Y. Q. Zhao, X. H. Zhao and W. K. Wang, *Chem. Eng. J.*, 2015, **266**, 74–81.

41 R. D. Shannon, *Acta Crystallogr., Sect. A: Cryst. Phys., Diffr., Theor. Gen. Crystallogr.*, 1976, **32**, 751–767.

42 M. Horsfall Jnr and E. Akporhonor, *Electron. J. Biotechnol.*, 2006, **9**, 6.

43 S. J. Kharat, *J. Mol. Liq.*, 2008, **140**, 10–14.

44 P. Xu and H. Xu, *ACS Omega*, 2019, **4**, 5848–5851.

45 B. G. Kwon, D. S. Lee, N. Kang and J. Yoon, *Water Res.*, 1999, **33**, 2110–2118.

46 M. Pettine, L. Campanella and F. J. Millero, *Environ. Sci. Technol.*, 2002, **36**, 901–907.

47 N. Nurnaeimah, N. Mat, K. Suryati Mohd, N. A. Badaluddin, N. Yusoff, M. H. Sajili, K. Mahmud, A. F. Mohd Adnan and M. M. Khandaker, *Agronomy*, 2020, **10**, 599.

48 R. Tarrahi, A. Movafeghi, A. Khataee, F. Rezanejad and G. Gohari, *Mol*, 2019, **24**, 410.

49 K. Wang, J. Cai, S. L. Xie, J. Feng and T. Wang, *Arch. Environ. Prot.*, 2015, **41**, 39–46.

50 K. Borowiak, M. Gąsecka, M. Mleczek, J. Dąbrowski, T. Chadzinikolau, Z. Magdziak, P. Goliński, P. Rutkowski and T. Kozubik, *Acta Physiol. Plant.*, 2015, **37**, 155.

51 T. V. Wagner, V. de Wilde, B. Willemsen, M. Mutaqin, G. Putri, J. Opdam, J. R. Parsons, H. H. M. Rijnaarts, P. de Voogt and A. A. M. Langenhoff, *J. Environ. Manage.*, 2020, **271**, 110972.

52 C. X. Mu, L. Wang and L. Wang, *Environ. Sci. Pollut. Res.*, 2020, **27**, 25140–25148.

53 L. H. Liu, T. Y. Chou, C. Y. Lee, D. J. Lee, A. Su and J. Y. Lai, *Int. J. Hydrogen Energy*, 2016, **41**, 4504–4508.

54 X. Y. Yong, D. Y. Gu, Y. D. Wu, Z. Y. Yan, J. Zhou, X. Y. Wu, P. Wei, H. H. Jia, T. Zheng and Y. C. Yong, *J. Hazard. Mater.*, 2017, **324**, 178–183.

55 H. Ilyas and E. D. van Hullebusch, *Water*, 2019, **11**, 2356.

56 I. Vera, N. Verdejo, W. Chávez, C. Jorquera and J. Olave, *J. Environ. Sci. Health, Part A*, 2016, **51**, 105–113.

57 C. C. Zhao, D. W. Shang, Y. L. Zou, Y. D. Du, Q. Wang, F. Xu, L. Ren and Q. Kong, *Sci. Total Environ.*, 2020, **732**, 139127.

58 P. Srivastava, A. K. Yadav, V. Garaniya, T. Lewis, R. Abbassi and S. J. Khan, *Sci. Total Environ.*, 2020, **698**, 134248.

59 Q. Wang, R. Lv, E. R. Rene, X. Y. Qi, Q. Hao, Y. D. Du, C. C. Zhao, F. Xu and Q. Kong, *Bioresour. Technol.*, 2020, **302**, 122867.

60 F. Zhong, C. M. Yu, Y. H. Chen, X. Wu, J. Wu, G. Y. Liu, J. Zhang, Z. F. Deng and S. P. Cheng, *Front. Microbiol.*, 2020, **11**, 1896.

61 H. L. Song, H. Li, S. Zhang, Y. L. Yang, L. M. Zhang, H. Xu and X. L. Yang, *Chem. Eng. J.*, 2018, **350**, 920–929.

62 H. Li, S. Zhang, X. L. Yang, Y. L. Yang, H. Xu, X. N. Li and H. L. Song, *Chemosphere*, 2019, **217**, 599–608.